Effect of modified corn stalk combined with ultrasonic conditioning on sludge dewatering performance

Feng Lin[a], Siqi Zhang[a], Jing Ma[b1], Shuxin Zhang[a], Baoyu Wang[a], Huanlei Yang[a]

[a] School of Chemical Engineering and Technology, Guangdong Industry Polytechnic University, Guangzhou, China

[b] Automotive Engineering Department, Jining Polytechnic, Jining, China

[1] Corresponding author at: Automotive Engineering Department, Jining Polytechnic, Jining, China

E-mail address: 15603052358@163.com (J. Ma)

Text S1

The plant employs the deep-water type improved A^2/O + rectangular treatment process. The sludge was concentrated to 94.50%-95% through gravity sedimentation, then stored in a refrigerator at 4°C for later use. Before usage, the sludge was thoroughly mixed and brought to room temperature. The wastewater treatment plant employs an enhanced A^2/O+ rectangular treatment process, with a hydraulic retention time (HRT) ranging from 8 to 12 hours and a sludge retention time (SRT) between 15 and 30 days. The effluent chemical oxygen demand (COD) concentration is maintained at 7–20 mg/L, with a removal rate of approximately over 90%. The effluent ammonia-nitrogen concentration is kept at 0.10–0.50 mg/L, achieving a removal rate of over 95%. The total nitrogen (TN) removal rate is around 70%–80%, while the total phosphorus (TP) concentration is relatively low, with a removal rate of approximately 60%–70%.

A 100 mL of sludge was poured into a 250 mL beaker, and a certain amount of MCSP was added at room temperature. The mixture was initially agitated at 150 rpm for 30 s, followed by stirring at 50 rpm for 2 min. Subsequently, the conditioned sludge was allowed to stand in the beaker for 10 min. Each test was conducted in triplicate.

One hundred milliliters of sludge was placed into a 250 mL beaker and subjected to ultrasonication at a frequency of 20 kHz and power intensity of 100 W for 10 min. Afterward, the dewatering agent MCSP was added to the sludge sample. The mixture

was initially agitated at 150 rpm for 30 s, followed by stirring at 50 rpm for 2 min. Subsequently, the conditioned sludge was allowed to stand in the beaker for 10 min. Each test was conducted in triplicate.

Text S2

In this study, the sludge dewatering performance was evaluated by measuring the water content of the dewatered sludge. The pressure applied during filtration was set at 5-6.0 MPa, and the filtration time was fixed at 5 min. The water content of the dewatered sludge was determined using a moisture analyzer (HX204, Mettler Toledo).

The specific resistance to filtration (SRF) of sludge represents the resistance per unit filtration area encountered by unit mass of sludge during filtration under a constant pressure. It stands as a pivotal indicator for assessing the filtration performance of sludge. Utilizing a Buchner funnel with an inner diameter of 7 cm, a sludge sample of 100 mL was subjected to suction filtration through rapid qualitative filter paper while maintaining a pressure of 0.05 MPa. The volumes of filtrate at corresponding time intervals were recorded and utilized to compute the SRF, with the calculation formula presented as follows:

$$r = \frac{2bPA^2}{\mu C}$$

where

r - Specific resistance to filtration of sludge, in meters per kilogram ($m \cdot kg^{-1}$);

b - The slope of the filtration equation $t/V = b \cdot V + a$, in seconds per meter to the power of negative six ($s \cdot m^{-6}$);

P - Pressure, in megapascals (MPa) or newtons per meter squared ($N \cdot m^{-2}$);

A - Filtration area, in meters squared (m^2);

μ - Viscosity of the filtrate, in newtons per second per meter squared ($N \cdot s \cdot m^{-2}$);

C - Mass of dry sludge retained by the filter paper per unit volume of filtrate, in kilograms per meter cubed ($kg \cdot m^{-3}$).

The bound water content of sludge flocs was determined using Differential Scanning Calorimetry (DSC). A certain amount of sludge precipitate, obtained after centrifuging at 1800 r/min for 5 minutes, was placed in a Differential Scanning Calorimeter (DSC 214, NETZSCH). The sample was cooled from room temperature to -25°C at a rate of -2°C/min and then heated back to 20°C at the same rate. The enthalpy change (ΔH) of the exothermic peak was obtained from the differential thermal curve, which was calibrated using ultrapure water of known mass. The calculation formula is as follows:

$$WB = WT - \Delta H/\Delta H0$$

where

WB - Bound water content (g/g DS);

WT - Total water content in the sludge cake (g/g DS);

ΔH - Enthalpy change during the endothermic process of the sludge cake (J/g);

ΔH0 - Enthalpy change during the endothermic process of ultrapure water (J/g).

Text S3

Initially, 45 mL of sludge was centrifuged at 4000 g for 5 min in a 50 mL centrifuge tube, and the supernatant obtained after filtration through a 0.45 μm membrane was designated as soluble EPS (S-EPS). The remaining precipitate was resuspended using 0.05% NaCl preheated to 65 °C to a volume of 45 mL, vortexed, and centrifuged again at 4000 g for 10 min. The supernatant obtained after filtration through a 0.45 μm membrane was designated as loosely bound EPS (LB-EPS). Subsequently, 0.05% NaCl at 65 °C was added to the precipitate to a volume of 45 mL, resuspended using a vortex mixer, heated in a water bath for 30 min, and centrifuged at 4000 g for 15 min. The supernatant obtained after filtration through a 0.45 μm membrane was designated as tightly bound EPS (TB-EPS).

Text S4

Image processing includes the following steps:

Image Acquisition: Microscopy was employed to capture images of sludge flocs.

Background Processing: The influence of background brightness, noise, and impurities during image capture was eliminated.

Image Segmentation: A thresholding technique was applied to convert the images into binary images. Based on the grayscale distribution characteristics of the captured images, the grayscale threshold range was adjusted to separate the flocs from the background.

Feature Extraction: Intrinsic parameter data of the measurement software, such as floc area, perimeter, and circularity, were utilized.

Data Analysis: The calculated results of the intrinsic parameters from the software were exported to an Excel file, where the values of the exported parameters were further computed.

The sludge floc was placed under a stereo microscope, and several images of the floc were captured. The captured images were processed using Image Pro Plus 6.0 software to calculate the projection area (A), perimeter (P), and major axis length (La). Based on the relationships $P \propto La^{D_1}$ and $A \propto P^{D_2}$, the one-dimensional fractal dimension (D_1) and two-dimensional fractal dimension (D_2) were obtained.

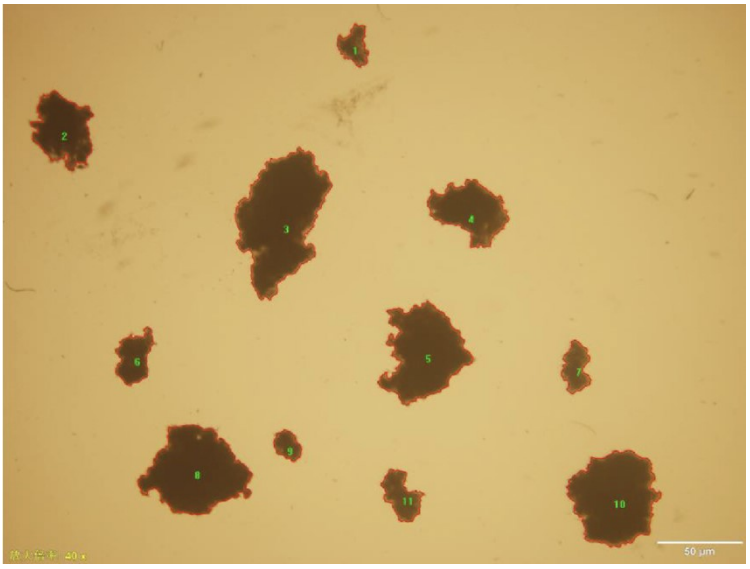

Text S5

In the 1500-1800 cm^{-1} region, the FTIR spectra of CSP and MCSP show significant differences. For CSP, the absorption peak at 1514 cm^{-1} corresponds to the C=C stretching vibration of aromatic rings, indicating the presence of aromatic compounds in CSP. The peak at 1730 cm^{-1} is attributed to the C=O stretching vibration, which may originate from ester or carbonyl compounds. After modification, the etherification reaction introduces ether bonds (C-O-C) and alkyl chains ($-CH_2-$), altering the molecular structure of CSP. As a result, a new peak appears at 1625.7 cm^{-1} in the FTIR spectrum of MCSP, primarily due to the introduction of amide or carboxyl groups by the etherification reaction, which manifests as a C=O stretching vibration peak at 1625.7 cm^{-1}. The etherification reaction likely increases the content of aliphatic compounds, evidenced by the C-H bending vibration peak at 1401 cm^{-1} in the FTIR spectrum. Additionally, the introduction of more ether bonds and alcoholic functional groups by the etherification reaction is indicated by the C-O stretching vibration peak at 1035.5 cm^{-1}. This further confirms that the etherification reaction

introduces quaternary ammonium groups, enhancing the cationic properties and surface charge distribution of cellulose, rendering MCSP positively charged. Thus, the addition of MCSP can facilitate electrostatic neutralization, which helps to adsorb and aggregate colloidal particles in the sludge system, thereby improving sludge dewatering performance.

Text S6

Influence of preparation conditions on sludge dewatering performance

Through single-factor experiments, the effects of alkali concentration, alkalization time, etherification temperature, etherification time, and etherification agent concentration during the preparation of MCSP on sludge dewatering performance were investigated. As shown in Fig. S3, with the increase in alkali concentration, both the SRF and the water content of the dewatered sludge initially decreased and then increased. When the alkalization concentration was 8%, the SRF and water content of the dewatered sludge decreased to 5.36×10^{12} m·kg^{-1} and 62.32%, respectively. However, when the alkalization concentration increased to 20%, the SRF and water content of the dewatered sludge rose to 7.45×10^{12} m·kg^{-1} and 66.31%, respectively. In the optimization experiment for alkalization time, when the alkalization time was 0.5 h, the SRF and water content of the dewatered sludge were 5.22×10^{12} m·kg^{-1} and 65.01%, respectively. Similarly, as the alkalization time increased, the SRF and water content of the dewatered sludge also showed an

increasing trend. This indicates that alkalization conditions have a significant impact on the properties of MCSP, which in turn plays a crucial role in sludge conditioning. This is because during the alkalization process, sodium ions and hydroxyl ions that are paired apart form hydrated ions (Choo et al., 2023). At lower alkali concentrations, these hydrated ions bind a large number of water molecules, resulting in excessive size that prevents them from effectively destroying the crystalline structure within the fiber crystal region. As the NaOH concentration increases, the number of water molecules that can form hydrated ions in the liquid phase decreases, thereby reducing the size of these hydrated ions and allowing them to penetrate into the fiber crystal region to participate in reactions. However, when the alkali concentration further increases, the size of these hydrated ions decreases further, reducing the efficiency of crystal region destruction, and the number of sodium ions contained therein also increases, competing with bound water, leading to a decrease in the swelling degree of the fiber structure (Feng et al., 2024).

During the etherification reaction, as the etherification temperature increased, the SRF and the water content of the dewatered sludge initially increased and then decreased. At an etherification temperature of 60°C, the SRF and water content reached their lowest values, which were 5.54×10^{12} $m\cdot kg^{-1}$ and 63.35%, respectively. Additionally, similar trends were observed for the effects of etherification time and etherification agent concentration on sludge dewatering. This is primarily due to the etherification treatment of corn stalk using the CTMAB, which results in the modified product surface carrying positive charges. These positive charges can neutralize the

166 negative charges contained in the sludge, disrupting the stable state of the sludge
167 system and facilitating subsequent mechanical removal of water, thereby improving
168 sludge dewatering performance. However, when the etherification concentration,
169 temperature, and time are excessive, leading to an excessive number of positive
170 charges on the surface of the modified product, an excessive number of positive
171 charges in the system can reform a stable system with opposite charges, which is
172 unfavorable for the occurrence of repolymerization reactions, thereby deteriorating
173 sludge dewatering performance.

174 **Optimization of preparation conditions using response surface methodology**

175 Based on the optimal value ranges of factors A (alkali concentration), B
176 (alkalization time), C (etherification temperature), and E (etherification concentration)
177 determined through single-factor experiments, the water content of the dewatered
178 sludge was selected as the response variable (R1). Utilizing the Box-Behnken design
179 of the response surface methodology (RSM) for a 5-factor, 3-level experimental
180 scheme, a total of 46 experimental trials were conducted.

181 As shown in Table S2 and Fig. S4, variance analysis and interaction analysis
182 were conducted on the regression equation for the moisture content of the sludge cake
183 after press filtration. The P-value indicates the significance within the model equation.
184 A regression "Prob > F" value and its corresponding value less than 0.0500 signify a
185 significant model term, whereas a value greater than 0.1000 indicates the opposite
186 (Liu et al., 2010). The quadratic model exhibited an F-value of 182.61 and a P-value <

187 0.0001, indicating a highly significant quadratic polynomial regression model.
188 Analysis of lack of fit for the quadratic polynomial revealed a "Lack of Fit" F-value
189 of 1.65, which is greater than 0.05, suggesting that the model's lack of fit is not
190 significant, which is beneficial for the model. The multiple correlation coefficient (R^2)
191 for the quadratic model was 0.98, indicating that 98% of the data variability in this
192 RSM statistical analysis can be explained by the model. Furthermore, the significance
193 test of the quadratic polynomial regression equation revealed that the primary terms,
194 including A (alkali concentration), B (alkalization time), C (etherification
195 temperature), and E (etherification concentration), had significant effects on the
196 sludge dewatering performance. The interaction terms AB, AE, BC, BD, and CE also
197 significantly influenced the response value. Among the quadratic terms, A^2, B^2, C^2,
198 D^2, and E^2 had extremely significant effects on the response value (Liu et al., 2010).

199 Additionally, based on the experimental results and the mathematical analysis of
200 the quadratic regression model, the optimal preparation parameters for MCSP were
201 determined as follows: A - alkali concentration of 10%, B - alkalization time of 1.083
202 h, C - etherification temperature of 60°C, D - etherification time of 2.083 h, and E -
203 etherification concentration of 50%. After five experiments, the water content of the
204 dewatered sludge was 54.3±2%, which was close to the theoretically predicted value.
205 This demonstrates that the use of the BBD method to optimize the preparation
206 conditions of MCSP can accurately fit the relationship between the response value
207 and the influencing factors, exhibiting high reliability.

208 **Text S7**

Due to the high crystallinity of cellulose in corn straw, an alkaline pretreatment is conducted prior to the etherification reaction. This process loosens the bonds between the components of the raw material, increases the amorphous regions, and enlarges the contact area between the reagents and the hydroxyl groups of cellulose in the raw material, thereby enhancing the reactivity of cellulose in corn straw. Subsequently, cetyltrimethylammonium bromide (CTMAB) is used for the etherification treatment to introduce quaternary ammonium groups, endowing the modified product with a positively charged surface.

218

219 **Table S1** Characteristics of the activated sludge

Parameter	Value
Water content (%)	95±0.30
SRF ($\times 10^{12} m \cdot kg^{-1}$)	9.35±0.3
Dv[50]（μm）	43.5±0.81
Zeta potential (mV)	-16.30±1.10
D1	1.23
D2	1.12
Bound water content (g/g DS)	8.53
pH	6.60±0.20
VSS (g/L)	4.3 ± 0.12

220

221 **Table S2 Response surface model analysis**

Source	Sum of squares	df	Mean squares	F-value	P-value	
Model	240.44	20	12.02	182.61	< 0.0001	significant
A-Alkali concentratio	5.49	1	5.49	83.33	< 0.0001	
B-Alkali treatment time	13.58	1	13.58	206.24	< 0.0001	

C-Etherification temperature	7.80	1	7.80	118.45	< 0.0001
D-Etherification time	0.5406	1	0.5406	8.21	0.0083
E-Etherification concentration	32.66	1	32.66	496.08	< 0.0001
AB	0.9025	1	0.9025	13.71	0.0011
AC	0.2070	1	0.2070	3.14	0.0884
AD	0.0009	1	0.0009	0.0132	0.9094
AE	1.06	1	1.06	16.12	0.0005
BC	6.73	1	6.73	102.29	< 0.0001
BD	8.73	1	8.73	132.64	< 0.0001
BE	0.0439	1	0.0439	0.6667	0.4219
CD	0.0000	1	0.0000	0.0000	1.0000
CE	0.6806	1	0.6806	10.34	0.0036
DE	0.0056	1	0.0056	0.0854	0.7725
A^2	25.80	1	25.80	391.92	< 0.0001
B^2	19.86	1	19.86	301.70	< 0.0001
C^2	34.60	1	34.60	525.51	< 0.0001
D^2	24.06	1	24.06	365.41	< 0.0001

E^2	152.87	1	152.87	2322.10	< 0.0001
Residual	1.65	25	0.0658		
Lack of Fit	1.65	20	0.0823		
Pure Error	0.0000	5	0.0000		
Cor Total	242.08	45			

222

223

224 **Table S3 Pearson correlation coefficient**

	WC	SPN	SPS	LBPN	LBPS	TBPN	TBPS	Dv[50]	ZP	D1	D2	BC
WC	1	-0.660	-0.641	-0.674	-0.652	-0.737	-0.741	-0.903*	-0.890*	0.690	-0.836*	0.921**
SPN		1	0.994**	0.988**	0.988**	0.986**	0.990**	0.597	0.921**	-0.995**	0.877*	-0.900*
SPS			1	0.985**	0.992**	0.971**	0.984**	0.553	0.900*	-0.998**	0.863*	-0.886*
LBPN				1	0.997**	0.965**	0.992**	0.558	0.927**	-0.987**	0.836*	-0.906*
LBPS					1	0.962**	0.989**	0.538	0.911*	-0.991**	0.841*	-0.893*
TBPN						1	0.986**	0.717	0.955**	-0.981**	0.939**	-0.936**
TBPS							1	0.653	0.960**	-0.992**	0.898*	-0.944**
Dv[50]								1	0.815*	-0.602	0.876*	-0.825*
ZP									1	-0.926**	0.932**	-0.994**
D1										1	-0.885*	0.915*
D2											1	-0.932**
BC												1

225

226

227

228 Table **S4** Characteristic values and cumulative contribution rates

	Initial eigenvalue			Extract sum of squares and load			Rotate the sum of squares to load		
Component	Eigenvalues	Variance %	Cumulative contribution rate %	Total	Variance %	Accumulate %	Total	Variance %	Accumulate %
1	10.02	91.12	91.12	10.0	91.118	91.118	7.28	66.21	66.21

2	0.83	7.56	98.68	0.83	7.564	98.682	3.55	32.30	98.51
3	0.11	0.998	99.68	0.11	0.998	99.680	0.13	1.17	99.68
4	0.025	0.23	99.91						

229

230

231 **Table S5 Component matrix**

Variables	Factor before rotation			Factor after rotation		
	F1	F2	F3	F1	F2	F3
SPN	0.981	-0.173	0.058	0.918	0.390	-0.017
SPS	0.971	-0.222	0.072	0.937	0.345	-0.032
LBPN	0.972	-0.216	-0.076	0.930	0.345	0.117
LBPS	0.969	-0.239	-.022	0.942	0.327	0.062
TBPN	0.993	-0.014	0.088	0.843	0.532	-0.045
TBPS	0.994	-0.100	-0.037	0.886	0.456	0.079
Dv[50]	0.726	0.686	0.018	0.235	0.971	0.019
ZP	0.975	0.159	-0.150	0.726	0.660	0.194
D1	-0.984	0.164	-0.042	-0.915	-0.399	0.001
D2	0.938	0.283	0.183	0.638	0.754	-0.139
BC	-0.964	-0.190	0.167	-0.699	-0.679	-0.210

232

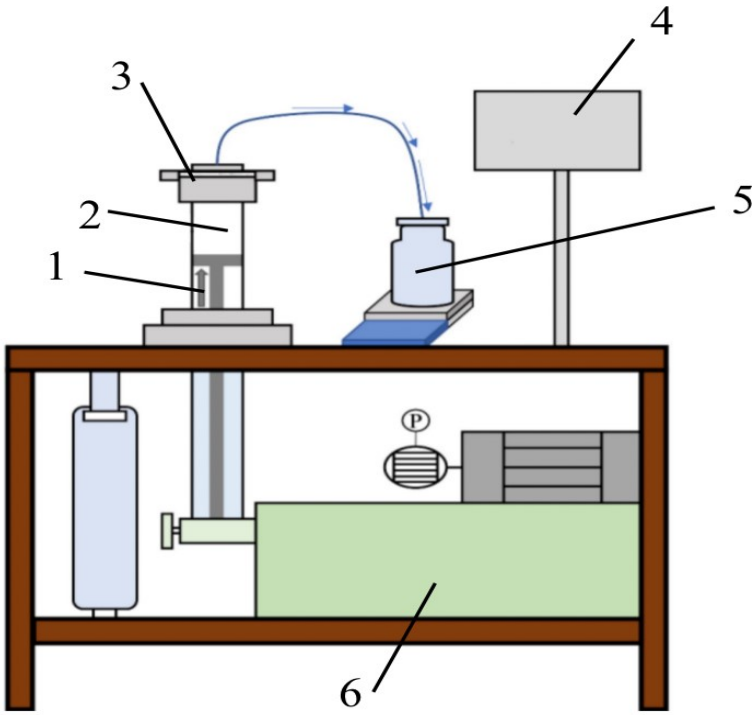

Fig. S1 Sludge filter press system

1 Stress direction; 2 press chamber; 3 Filter cloth; 4 The control panel; 5 The filtrate bottle; 6 The hydraulic system

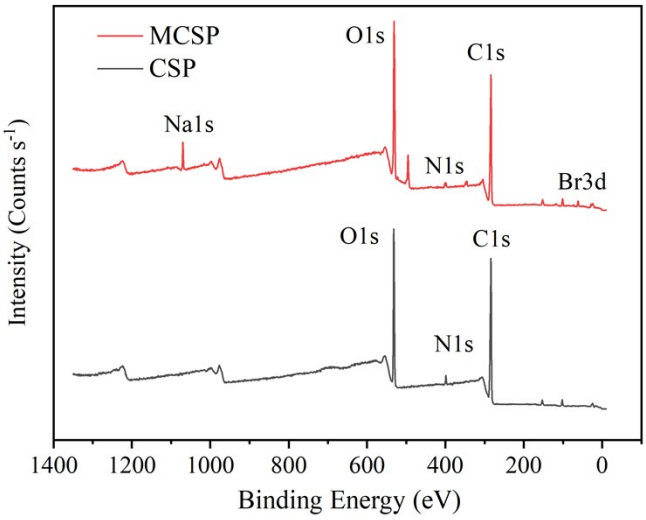

240

241

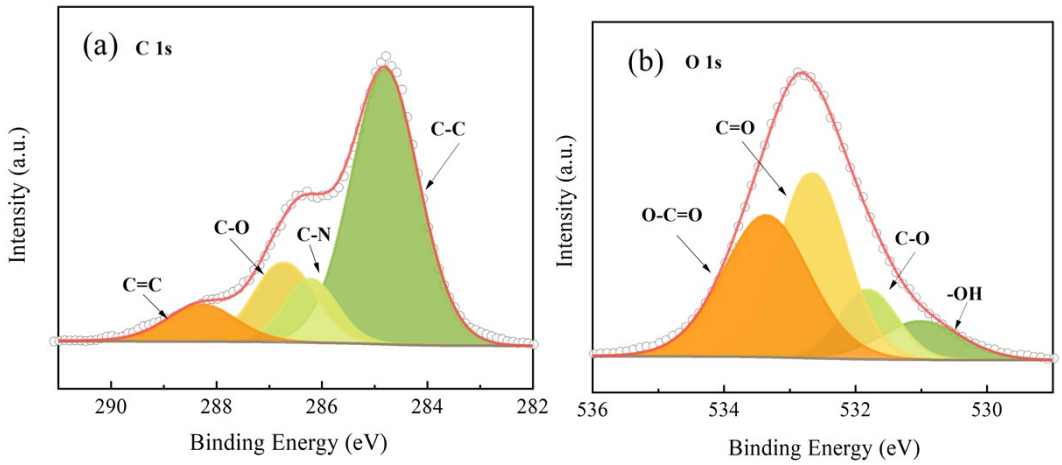

242

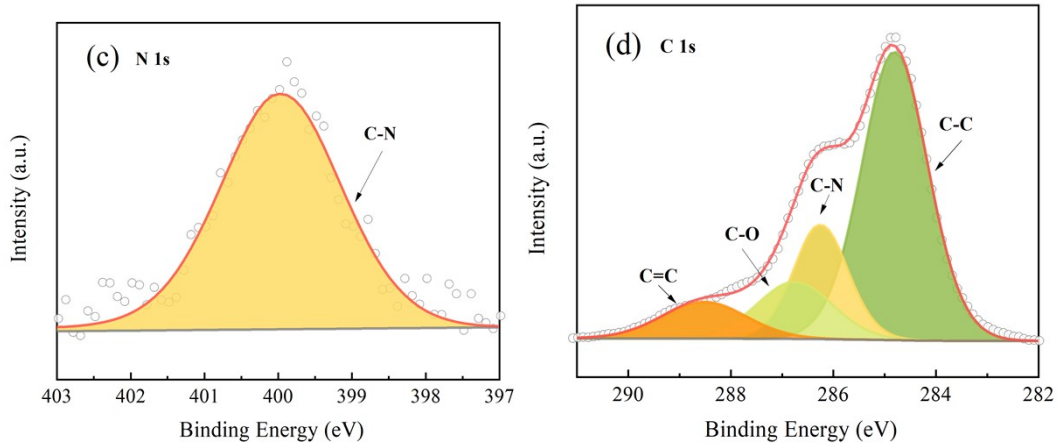

243

244

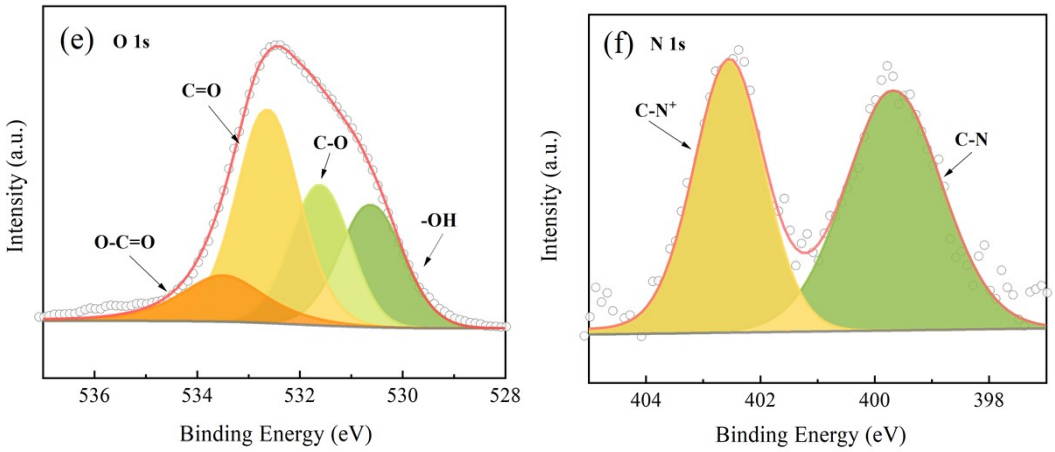

245

246 **Fig. S2 XPS-wide scans of the CSP and the MCSP**

247

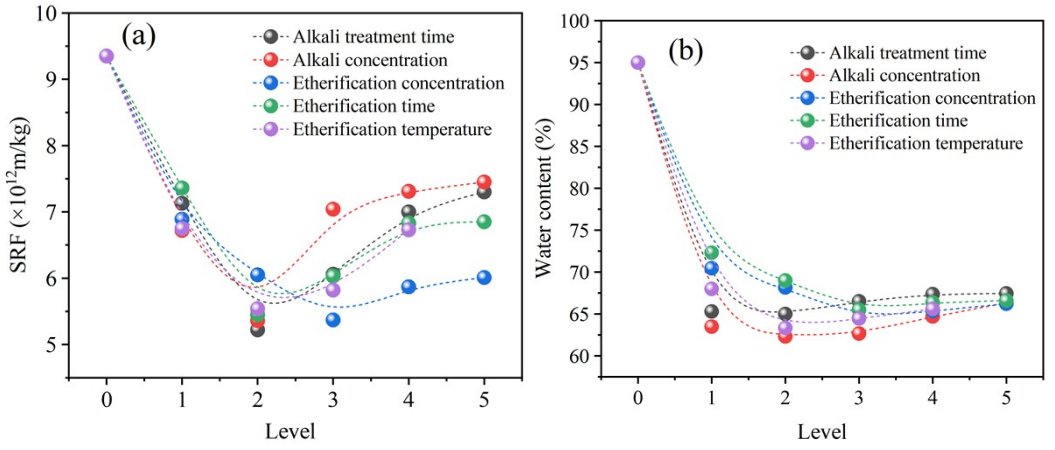

248

249

250 **Fig. S3 Impact of preparation conditions of MCSP on sludge dewatering**

251 **performance**

252 **(a) Alkali Concentration; (b) Alkalization Time; (c) Etherification Temperature;**

253 **(d) Etherification Time; (e) Etherification Agent Concentration**

254

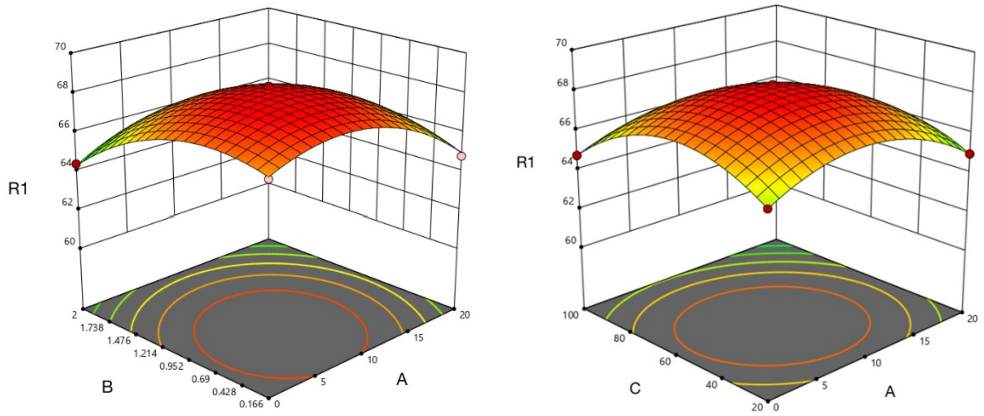
R1
70
68
66
64
62
60
B
2
1.738
1.476
1.214
0.952
0.69
0.428
0.166
A
0
5
10
15
20
C
100
80
60
40
20

255

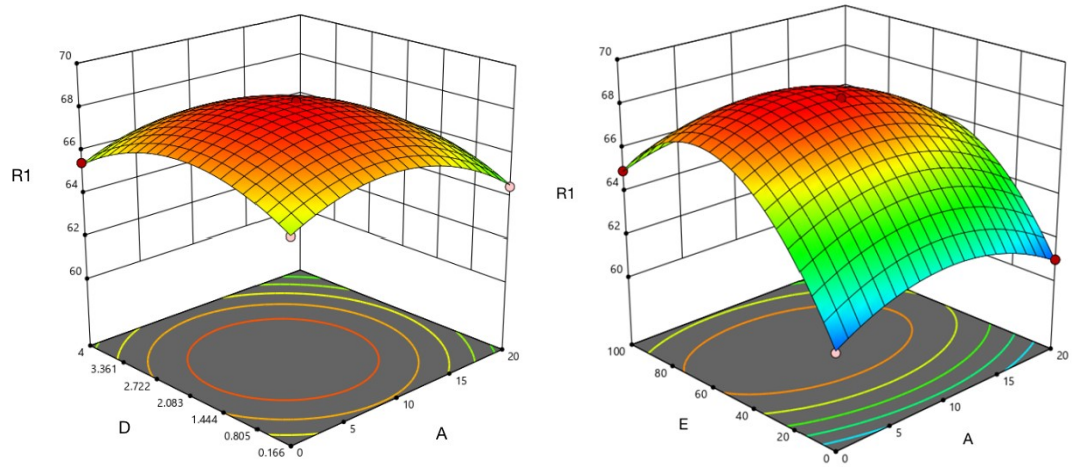
R1
70
68
66
64
62
60
D
4
3.361
2.722
2.083
1.444
0.805
0.166
A
0
5
10
15
20
E
100
80
60
40
20
0

256

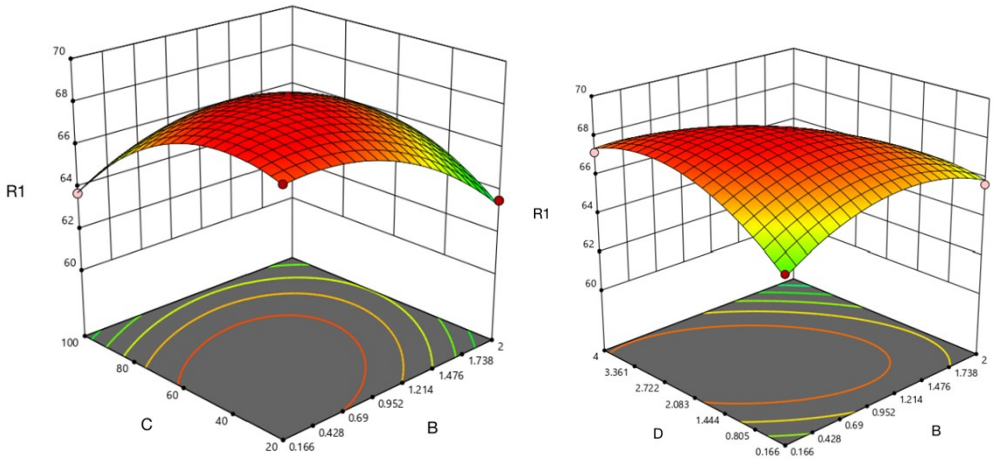
R1
70
68
66
64
62
60
C
100
80
60
40
20
B
0.166
0.428
0.69
0.952
1.214
1.476
1.738
2
D
4
3.361
2.722
2.083
1.444
0.805
0.166

257

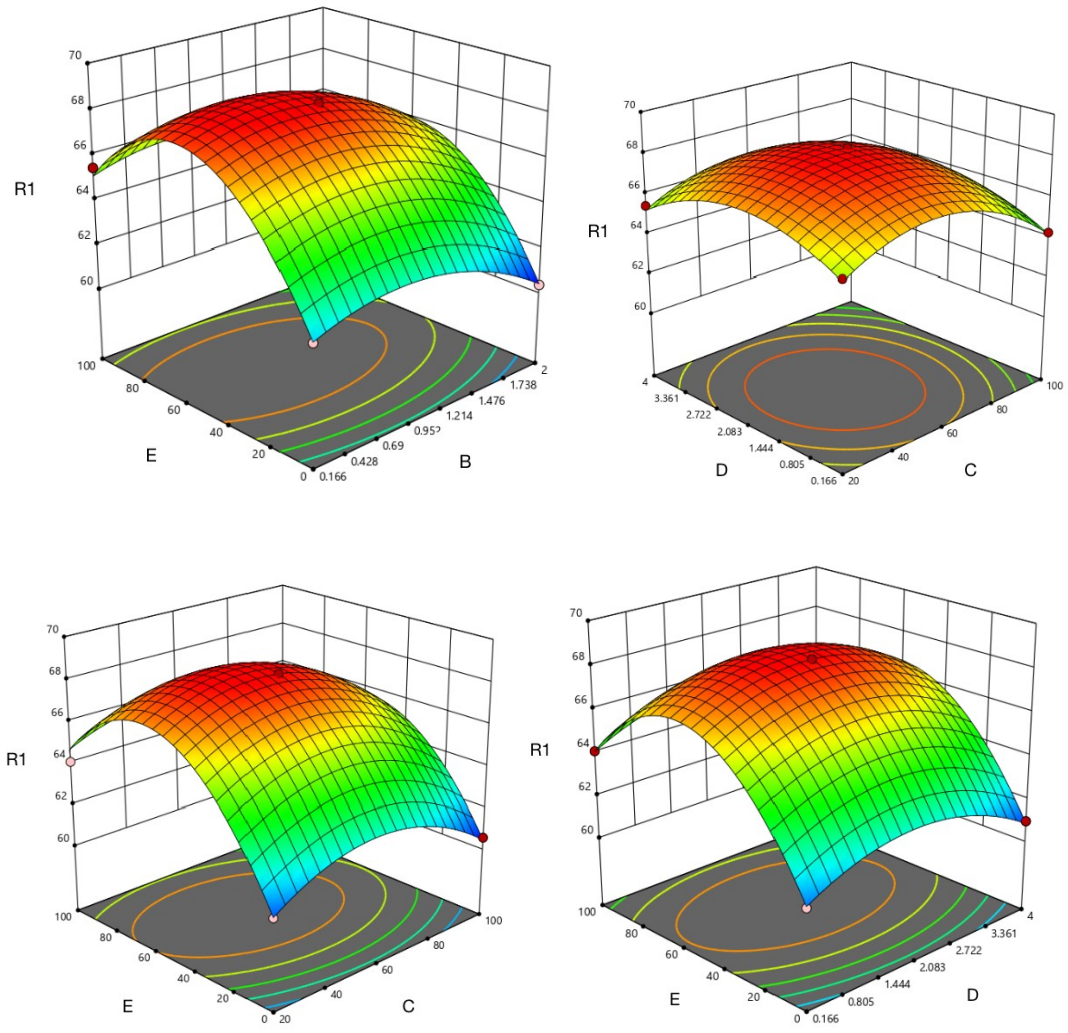

Fig. S4 Interaction analysis of response surface

A-Alkali concentration; B-Alkali treatment time; C-Etherification temperature; D-Etherification time; E-Etherification concentration

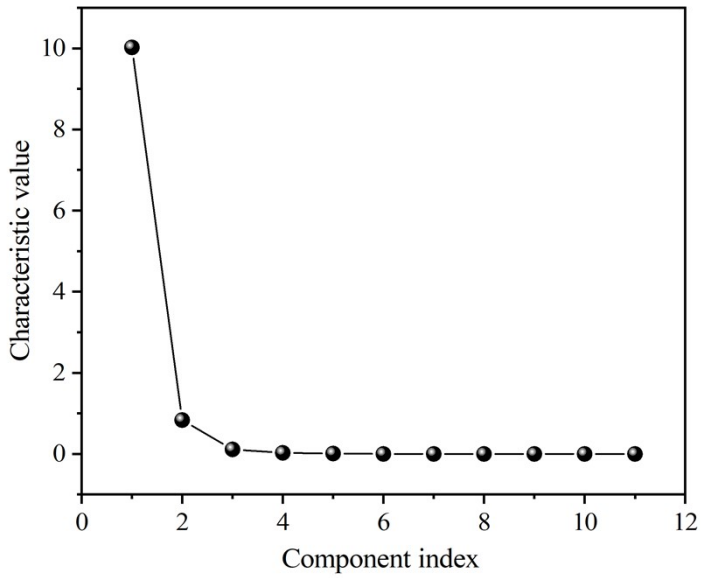

267

268 **Fig. S5 Scree plot**

269

270

271

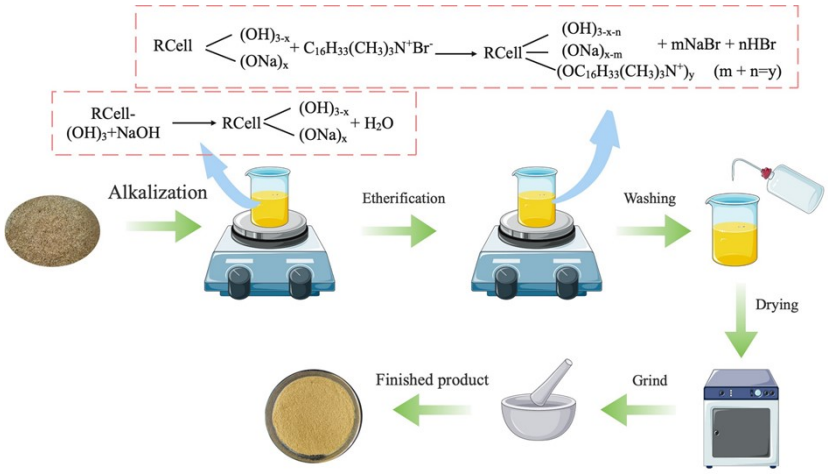

272

273 **Fig. S6 Preparation of MCSP**

274

275

276

277 Choo T F, Saidin N U, Zali N M, Azhar N (2023) Electrocatalytic and photocatalytic
278 activities of hierarchically structured zinc oxide nanoparticles derived from
279 cellulose paper-precipitated hydrozincite. Ceram Int 49 39180-39188.
280 https://doi.org/10.1016/j.ceramint.2023.09.261

281 Feng Z, Yang Z, Cao J, Wu Z, Gai E, Wu L (2024) Flocculation of kaolin and anion
282 dye by cationic cellulose-based flocculant: RSM-optimized synthesis and
283 experimental study. J Environ Chem Eng 12 112309.
284 https://doi.org/10.1016/j.jece.2024.112309

285 Liu Y, Zheng Y, Wang A (2010) Response surface methodology for optimizing
286 adsorption process parameters for methylene blue removal by a hydrogel
287 composite. Adsorp Sci Technol 28 913-922. https://doi.org/10.1260/0263-
288 6174.28.10.913

289